

# Error Analysis of Feature Based Disparity Estimation

Patrick A. Mikulastik, Hellward Broszio, Thorsten Thormählen, and Onay Urfalioglu

Information Technology Laboratory, University of Hannover, Germany  
{mikulast, broszio, thormae, urfaliog}@lfi.uni-hannover.de  
<http://www.lfi.uni-hannover.de>

**Abstract.** For real-time disparity estimation from stereo images the coordinates of feature points are evaluated. This paper analyses the influence of camera noise on the accuracy of feature point coordinates of a feature point detector similar to the *Harris Detector*, modified for disparity estimation. As a result the error variance of the horizontal coordinate of each feature point and the variance of each corresponding disparity value is calculated as a function of the image noise and the local intensity distribution. Disparities with insufficient accuracy can be discarded in order to ensure a given accuracy. The results of the error analysis are confirmed by experimental results.

## 1 Introduction

Disparity estimation algorithms compute disparities from the coordinates of selected corresponding feature points from images in standard stereo geometry. For the use of these estimated disparities in computer vision systems it is desirable to specify their accuracy. Therefore, in this paper the error variance of a disparity estimator is determined analytically and experimentally.

In previous work Luxen [1] measures the variance of feature point coordinates, taking image noise into account. The result is a mean error variance of all feature points in an image at a specific level of image noise. Local intensity distributions at specific feature points are not taken into account. Rohr [2] introduces an analytical model of a corner and calculates the feature point coordinates of different feature detectors for this corner. Thus he characterizes the different detectors but does not consider the errors of the coordinates due to camera noise. Szeliski [3] has analytically calculated the accuracy of displacement estimators like the KLT-Tracker [4]. The resulting covariance matrix describes the variance of the displacement error for each displacement. Other approaches do not estimate displacements but nevertheless apply similar covariance matrices to describe the accuracy of feature point coordinates [5–8]. However, these results have not been analytically proven or evaluated in experiments. Thus, so far the accuracy of feature point coordinates from image gradient based detectors similar to the *Harris Detector* [9] has not been calculated analytically.

This paper analyses the influence of camera noise on the accuracy of a feature point detector for disparity estimation. It is based on a modified *Harris Detector* [9]. The accuracy is defined by the error variance of the feature coordinate. In a second step the error variance of the disparity estimation is derived.

In section 2 the feature detector considered in this paper is described. In section 3 an error analysis for feature coordinates and disparity is presented. Section 4 describes experiments for measuring the error variance of feature coordinates. Conclusions are given in section 5.

## 2 Feature Point Detector

The feature detector considered in this paper is based on the *Harris Detector* [9]. In stereo vision only disparities in horizontal direction of the stereo image are considered. Therefore, the process of feature detection is simplified so that only gradients in direction of the x-axis are measured. This also results in a reduced computational complexity.

For detection of feature points the following equation describes the edge response function  $R$  for vertical edges:

$$R(x, y) = \left| \sum_{i=-1}^1 I_x(x, y + i) \alpha_i \right|, \quad \alpha_i = [1, 2, 1] \quad (1)$$

where  $x$  and  $y$  are coordinates in the image.  $I_x$  is an approximation of the horizontal intensity gradient:

$$I_x(x, y) = -I(x - 2, y) - 2I(x - 1, y) + 2I(x + 1, y) + I(x + 2, y) \quad (2)$$

A feature point is detected, if  $R(x, y)$  is greater than a predefined threshold  $T_R$  and if  $R(x_m, y_m)$  is a local maximum in horizontal direction:

$$\begin{aligned} R(x_m, y_m) &> T_R \\ R(x_m, y_m) &> R(x_m - 1, y_m) \\ R(x_m, y_m) &> R(x_m + 1, y_m) \end{aligned} \quad (3)$$

**Estimation of subpel coordinates** In horizontal direction a subpel coordinate is estimated for every feature point. A parabola is fitted to the edge response function (see figure 1):

$$R(x, y) = a + bx + \frac{1}{2}cx^2 \quad (4)$$

To achieve a compact notation the coordinate system is chosen so that  $x_m = 0$ . The three parameters  $a, b, c$  are calculated with:

$$\begin{aligned} R(-1, y_m) &= a - b + \frac{1}{2}c \\ R(0, y_m) &= a \\ R(+1, y_m) &= a + b + \frac{1}{2}c \end{aligned} \quad (5)$$

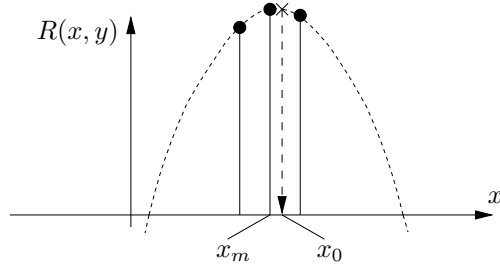
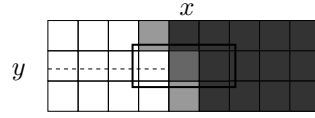


**Fig. 1.** Interpolation of  $R(x, y)$  with a parabola. The maximum defines the subpel coordinate of the feature point  $x_0$ .

Solved for  $a, b, c$ :

$$\begin{aligned}
 a &= R(0, y_m) \\
 b &= \frac{1}{2} (R(+1, y_m) - R(-1, y_m)) \\
 c &= R(-1, y_m) - 2R(0, y_m) + R(+1, y_m)
 \end{aligned} \tag{6}$$

In order to find the maximum of the parabola the derivation of equation 4 is set to zero:

$$\frac{\partial R(x, y)}{\partial x} = b + cx \stackrel{!}{=} 0 \tag{7}$$

The null of equation 7 marks the subpel coordinate  $x_0$  of the feature point:

$$\begin{aligned}
 x_0 &= -\frac{b}{c} \\
 &= \frac{1}{2} \frac{R(-1, y_m) - R(+1, y_m)}{R(-1, y_m) - 2R(0, y_m) + R(+1, y_m)}
 \end{aligned} \tag{8}$$

### 3 Variance of the horizontal coordinate

To consider the influence of image noise on the subpel coordinates of feature points, noisy intensity values  $\tilde{I}(x, y)$  with:

$$\tilde{I}(x, y) = I(x, y) + n(x, y) \tag{9}$$

are considered.  $n(x, y)$  is white, mean free and Gaussian distributed noise with a noise variance of  $\sigma_n^2$ . The gradient of the image noise is defined as:

$$n_x(x, y) = -n(x-2, y) - 2n(x-1, y) + 2n(x+1, y) + n(x+2, y) \quad (10)$$

Therefore, the measured image gradient is  $\tilde{I}_x(x, y)$ :

$$\begin{aligned} \tilde{I}_x(x, y) &= -\tilde{I}(x-2, y) - 2\tilde{I}(x-1, y) + 2\tilde{I}(x+1, y) + \tilde{I}(x+2, y) \\ &= I_x(x, y) \underbrace{-n(x-2, y) - 2n(x-1, y) + 2n(x+1, y) + n(x+2, y)}_{n_x(x, y)} \\ &= I_x(x, y) + n_x(x, y) \end{aligned} \quad (11)$$

The measured cornerness response function  $\tilde{R}(x, y)$  can be written as:

$$\begin{aligned} \tilde{R}(x, y) &= \left| \sum_{i=-1}^1 \tilde{I}_x(x, y+i) \alpha_i \right| \\ &= \left| \sum_{i=-1}^1 I_x(x, y+i) \alpha_i + \sum_{i=-1}^1 n_x(x, y+i) \alpha_i \right| \end{aligned} \quad (12)$$

$I_x$  can be positive or negative if the edge has a gradient in the positive or in the negative direction. The influence of the image noise is the same in both cases. Therefore only edges with positive gradients are considered in the following calculations and it is assumed that  $I_x$  is always positive:

$$\sum_{i=-1}^1 I_x(x, y+i) \alpha_i > 0 \quad (13)$$

Generally, the intensity values are much larger than the image noise:

$$\sum_{i=-1}^1 I_x(x, y+i) \alpha_i > \sum_{i=-1}^1 n_x(x, y+i) \alpha_i \quad (14)$$

With equations 13 and 14  $\tilde{R}(x, y)$  can be written as:

$$\tilde{R}(x, y) = \underbrace{\left| \sum_{i=-1}^1 I_x(x, y+i) \alpha_i \right|}_{R(x, y)} + \underbrace{\sum_{i=-1}^1 n_x(x, y+i) \alpha_i}_{R_n(x, y)} \quad (15)$$

with:

$$R_n(x, y) = \sum_{i=-1}^1 n_x(x, y+i) \alpha_i \quad (16)$$

$\tilde{R}(x, y)$  is computed for every point-position. The calculation of the feature point's subpel coordinates is carried out according to equation 3 to 7.  $\tilde{x}_0$  can be calculated with equation 8:

$$\tilde{x}_0 = \frac{1}{2} \frac{\tilde{R}(-1, y_m) - \tilde{R}(1, y_m)}{\tilde{R}(-1, y_m) - 2\tilde{R}(0, y_m) + \tilde{R}(1, y_m)} \quad (17)$$

and:

$$\tilde{x}_0 = \frac{1}{2} \frac{\tilde{R}(-1, y_m) - \tilde{R}(1, y_m)}{c + \underbrace{R_n(-1, y_m) - 2R_n(0, y_m) + R_n(1, y_m)}_{\Delta c}} \quad (18)$$

For a more compact notation  $\Delta c$  is introduced:

$$\Delta c = R_n(-1, y_m) - 2R_n(0, y_m) + R_n(1, y_m) \quad (19)$$

as well as the normalized value  $\Delta c'$ :

$$\Delta c' = \frac{\Delta c}{c} \quad (20)$$

$c$  is a sum of intensity values and  $\Delta c$  is a sum of noise values. Therefore  $\Delta c'$  is a small value. With  $\Delta c$  and  $\Delta c'$  equation 18 simplifies to:

$$\begin{aligned} \tilde{x}_0 &= \frac{1}{2} \frac{\tilde{R}(-1, y_m) - \tilde{R}(1, y_m)}{c + \Delta c} \\ &= \frac{1}{2} \frac{\tilde{R}(-1, y_m) - \tilde{R}(1, y_m)}{c(1 + \Delta c')} \end{aligned} \quad (21)$$

Multiplication of nominator and denominator with  $(1 - \Delta c')$  equals to:

$$\tilde{x}_0 = \frac{1}{2} \frac{\tilde{R}(-1, y_m) - \tilde{R}(1, y_m)}{c(1 - \Delta c'^2)} - \frac{1}{2} \frac{\tilde{R}(-1, y_m) - \tilde{R}(1, y_m)}{c(1 - \Delta c'^2)} \cdot \Delta c' \quad (22)$$

Since  $\Delta c'$  is a small value it can be assumed that

$$1 \gg \Delta c'^2 \quad (23)$$

With this assumption, equation 22 is simplified to:

$$\tilde{x}_0 \approx \frac{1}{2} \frac{\tilde{R}(-1, y_m) - \tilde{R}(1, y_m)}{c} - \frac{1}{2} \frac{\tilde{R}(-1, y_m) - \tilde{R}(1, y_m)}{c} \cdot \Delta c' \quad (24)$$

With equation 16:

$$\begin{aligned} \tilde{x}_0 &\approx \overbrace{\left( \frac{R(-1, y_m) - R(1, y_m)}{2c} \right)}^{x_0} + \overbrace{\left( \frac{R_n(-1, y_m) - R_n(1, y_m)}{2c} \right)}^{\Delta x_a} \\ &\quad - \left( \frac{R(-1, y_m) - R(1, y_m)}{2c} + \frac{R_n(-1, y_m) - R_n(1, y_m)}{2c} \right) \cdot \Delta c' \end{aligned} \quad (25)$$

$\Delta x_a$  is defined:

$$\Delta x_a = \left( \frac{R_n(-1, y_m) - R_n(1, y_m)}{2c} \right) \quad (26)$$

With  $\Delta x_a$  we can write:

$$\tilde{x}_0 = x_0 + \Delta x_a - x_0 \Delta c' - \Delta x_a \Delta c' \quad (27)$$

$\Delta x_a \Delta c'$  is the product of sums of noise values. Therefore it is very small. It will be neglected in the following calculation:

$$\tilde{x}_0 = x_0 + \underbrace{\Delta x_a - x_0 \Delta c'}_{\Delta x_0} \quad (28)$$

$\Delta x_0$  describes the error of the undistorted coordinate  $x_0$ :

$$\Delta x_0 = \Delta x_a - x_0 \Delta c' \quad (29)$$

It has been verified that experimentally that  $\Delta x_0$  has a zero mean. With this assumption the variance of the coordinate's error  $\sigma_\Delta^2$  equals the root mean square  $E[\Delta x_0^2]$ :

$$\begin{aligned} \sigma_\Delta^2 &= E[\Delta x_0^2] = E[(\Delta x_a - x_0 \Delta c')^2] \\ &= E[\Delta x_a^2 - 2x_0 \Delta x_a \Delta c' + x_0^2 \Delta c'^2] \\ &= E[\Delta x_a^2] - E[2x_0 \Delta x_a \Delta c'] + E[x_0^2 \Delta c'^2] \end{aligned} \quad (30)$$

The terms of equation 30 are evaluated individually:

$$\begin{aligned} E[\Delta x_a^2] &= E\left[\left(\frac{R_n(-1, y_m) - R_n(1, y_m)}{2c}\right)^2\right] \\ &= \frac{1}{4c^2} E[(R_n(-1, y_m) - R_n(1, y_m))^2] \end{aligned} \quad (31)$$

With equation 15:

$$E[\Delta x_a^2] = \frac{1}{4c^2} E\left[\left(\sum_{i=-1}^1 n_x(-1, y_m + i) \alpha_i - \sum_{i=-1}^1 n_x(1, y_m + i) \alpha_i\right)^2\right]$$

Evaluation of the square gives:

$$\begin{aligned} E[\Delta x_a^2] &= \frac{1}{4c^2} E\left[\left(\sum_{i=-1}^1 n_x(-1, y_m + i) \alpha_i\right)^2 - 2 \sum_{i=-1}^1 n_x(-1, y_m + i) \alpha_i \cdot \right. \\ &\quad \left. \sum_{i=-1}^1 n_x(1, y_m + i) \alpha_i + \left(\sum_{i=-1}^1 n_x(1, y_m + i) \alpha_i\right)^2\right] \end{aligned} \quad (32)$$

With  $E[n(x, y_1)n(x, y_2)] = 0$ , for  $y_1 \neq y_2$  and  $E[n(x_1, y)n(x_2, y)] = 0$ , for  $x_1 \neq x_2$ :

$$\begin{aligned}
& E \left[ \left( \sum_{i=-1}^1 n_x(x, y+i) \alpha_i \right)^2 \right] \\
&= E \left[ \sum_{i=-1}^1 n_x^2(x, y+i) \alpha_i^2 \right] \\
&= E \left[ \sum_{i=-1}^1 (n^2(x-2, y+i) + 4n^2(x-1, y+i) + 4n^2(x+1, y+i) \right. \\
&\quad \left. + n^2(x+2, y+i)) \alpha_i^2 \right]
\end{aligned} \tag{33}$$

and

$$\begin{aligned}
& E \left[ \sum_{i=-1}^1 n_x(-1, y+i) \alpha_i \cdot \sum_{i=-1}^1 n_x(1, y+i) \alpha_i \right] \\
&= E \left[ \sum_{i=-1}^1 n_x(-1, y+i) \cdot n_x(1, y+i) \alpha_i^2 \right] \\
&= E \left[ \sum_{i=-1}^1 -4n^2(0, y+i) \alpha_i^2 \right].
\end{aligned} \tag{34}$$

Equation 32 simplifies to:

$$\begin{aligned}
E[\Delta x_a^2] &= \frac{1}{4c^2} E \left[ \sum_{i=-1}^1 (n^2(-3, y_m+i) + 4n^2(-2, y_m+i) + 4n^2(0, y_m+i) \right. \\
&\quad \left. + n^2(1, y_m+i)) \alpha_i^2 - 2 \sum_{i=-1}^1 -4n^2(0, y_m+i) \alpha_i^2 \right. \\
&\quad \left. + \sum_{i=-1}^1 (n^2(-1, y+i) + 4n^2(0, y+i) + 4n^2(2, y+i) \right. \\
&\quad \left. + n^2(3, y+i)) \alpha_i^2 \right]
\end{aligned} \tag{35}$$

For the expectation the terms  $n^2(x, y)$  become the variance of the image noise  $\sigma_n^2$ :

$$E[\Delta x_a^2] = \frac{1}{4c^2} \left[ \sum_{i=-1}^1 10\sigma_n^2 \alpha_i^2 - 2 \left( \sum_{i=-1}^1 -4\sigma_n^2 \alpha_i^2 \right) + \sum_{i=-1}^1 10\sigma_n^2 \alpha_i^2 \right] \tag{36}$$

Evaluation of the sums gives:

$$E[\Delta x_a^2] = \frac{\sigma_n^2}{4c^2} [60 + 48 + 60] = \frac{42\sigma_n^2}{c^2} \tag{37}$$

The second term in equation 30 can be expanded to:

$$\begin{aligned}
E[2\Delta x_a x_0 \Delta c'] &= E \left[ 2 \left( \frac{R_n(-1, y_m) - R_n(1, y_m)}{2c} \right) x_0 \frac{\Delta c}{c} \right] \\
&= E \left[ 2 \left( \frac{R_n(-1, y_m) - R_n(1, y_m)}{2c} \right) \right. \\
&\quad \left. x_0 \left( \frac{R_n(-1, y_m) - 2R_n(0, y_m) + R_n(1, y_m)}{c} \right) \right] \quad (38) \\
&= \frac{x_0}{c^2} E [(R_n(-1, y_m) - R_n(1, y_m)) \\
&\quad (R_n(-1, y_m) - 2R_n(0, y_m) + R_n(1, y_m))]
\end{aligned}$$

A calculation similar to that from equation 31 to 36 leads to:

$$\begin{aligned}
E[2\Delta x_a x_0 \Delta c'] &= \frac{x_0}{c^2} \left[ \sum_{i=-1}^1 10\sigma_n^2 \alpha_i^2 - \sum_{i=-1}^1 10\sigma_n^2 \alpha_i^2 \right] \cdot \\
&\quad \left[ -2 \left( \sum_{i=-1}^1 4\sigma_n^2 \alpha_i^2 \right) + 2 \left( \sum_{i=-1}^1 4\sigma_n^2 \alpha_i^2 \right) \right] \quad (39) \\
&= 0
\end{aligned}$$

The third term in equation 30 can be expanded to:

$$E \left[ x_0^2 \Delta c'^2 \right] = \frac{x_0^2}{c^2} E \left[ (R_n(-1, y_m) - 2R_n(0, y_m) + R_n(1, y_m))^2 \right] \quad (40)$$

Once again, a calculation similar to that from equation 31 to 36 leads to:

$$E \left[ x_0^2 \Delta c'^2 \right] = \frac{120\sigma_n^2 x_0^2}{c^2} \quad (41)$$

Insertion of equations 37, 39 and 41 in equation 30 leads to:

$$\begin{aligned}
\sigma_\Delta^2 &= \frac{42\sigma_n^2}{c^2} + \frac{120\sigma_n^2 x_0^2}{c^2} \\
&= \sigma_n^2 \frac{42 + 120x_0^2}{c^2} \quad (42) \\
&= \sigma_n^2 \frac{42 + 120x_0^2}{(R(-1, y_m) - 2R(0, y_m) + R(+1, y_m))^2}
\end{aligned}$$

This equation will be used to calculate the error variance  $\sigma_\Delta^2$  of the feature point coordinate. The disparity  $d$  is the distance between a feature point in the left image and the corresponding feature point in the right image:

$$d = x_{\text{left}} - x_{\text{right}} \quad (43)$$



The variance  $\sigma_{\Delta_d}^2$  of the disparity error  $\Delta d$  is:

$$\begin{aligned}
E[\Delta d^2] &= \sigma_{\Delta_d}^2 = E\left[\left(\Delta x_{\text{left}} - \Delta x_{\text{right}}\right)^2\right] \\
&= E\left[\Delta x_{\text{left}}^2 - 2\Delta x_{\text{left}}\Delta x_{\text{right}} + \Delta x_{\text{right}}^2\right] \\
&= E\left[\Delta x_{\text{left}}^2\right] - E\left[2\Delta x_{\text{left}}\Delta x_{\text{right}}\right] + E\left[\Delta x_{\text{right}}^2\right]
\end{aligned} \tag{44}$$

The distortions of the feature point's coordinates in the two images are statistically independent, therefore equation 44 simplifies to:

$$\begin{aligned}
\sigma_{\Delta_d}^2 &= E\left[\Delta x_{\text{left}}^2\right] + E\left[\Delta x_{\text{right}}^2\right] \\
&= \sigma_{\Delta_{\text{left}}}^2 + \sigma_{\Delta_{\text{right}}}^2
\end{aligned} \tag{45}$$

The variance of the disparity error is given by the sum of the error variances of the feature point coordinates.

## 4 Experimental Results

The following experiments have been carried out to evaluate the derivation from the preceding chapter 3. An image sequence consisting of a static scene with constant lighting is taken with a 3-Chip CCD camera (Sony DXC-D30WSP). In order to determine the size of  $\sigma_n^2$  the average intensity value at each pixel from 1000 frames is calculated to produce a noise free image for the sequence. By subtraction of the noise free image and the original images, difference images containing only the camera noise can be obtained. A camera noise variance of  $\sigma_n^2 = 4.8$  which equals a PSNR of 41.3 dB was measured for the sequence. Figure 2 shows an example of an image from the sequence.

Using the feature detector described in section 2 feature points are detected in every image of the sequence. Now, correspondences between the feature points in the sequence are established. A correspondence is given, if a feature point in one image is located at the coordinates  $x, y$  and in another image at the coordinates  $x \pm \epsilon, y \pm \epsilon$ , with  $\epsilon \leq 0,5$  pel. If a feature point has correspondences in all images of a sequence, the measured variance of its horizontal coordinate  $\tilde{\sigma}_{\Delta}^2$  is calculated. This value can be compared with the results from the derivation in section 3.

Figure 3 shows the measured variances  $\tilde{\sigma}_{\Delta}^2$  over the variances  $\sigma_{\Delta}^2$  calculated as described in section 3. The figure shows that the measured variances  $\tilde{\sigma}_{\Delta}^2$  have nearly the same values as the calculated ones. Therefore the calculation is confirmed by the experiment. Also the values lie in the same regions observed by other researchers [1].

A second experiment with a synthetic image shows the dependence between subpel position of a feature point and the error variance of its coordinate. The image shown in figure 4 is used for this experiment. A feature detection in this image results in feature points with subpel positions in the whole range  $-0.5 < x_0 < 0.5$  because the edge in the image is slightly slanted.

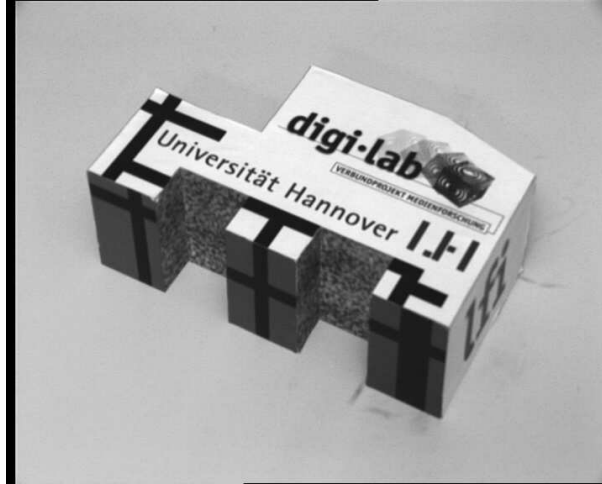


Fig. 2. Example image from the test sequence with a camera noise variance of  $\sigma_n^2 = 4.8$

Because the image shown in figure 4 is noise-free, synthetic noise was added to the image's intensity values to generate 1000 noisy images with the original image as a basis. Now the same procedure to calculate  $\tilde{\sigma}_\Delta^2$  and  $\sigma_\Delta^2$  as described with the real image is conducted.

Figure 5 shows the measured and the calculated noise variances of the feature point's coordinates  $\tilde{\sigma}_\Delta^2$  and  $\sigma_\Delta^2$  over the subpel coordinate. It can be observed that the coordinate error variance of feature points at a full-pel position is smaller than that for feature points at half-pel position. The variances vary by a factor of about three. Also, it can be observed that the calculated variances  $\sigma_\Delta^2$  match the measured variances  $\tilde{\sigma}_\Delta^2$ , which supports the correctness of the calculation.

## 5 Conclusions

A feature point detector using horizontal intensity gradients and offering subpel accuracy was described in section 2. It was shown that typically most of the feature points have an error variance of less than  $0.01\text{pel}^2$  for the horizontal coordinate. An analysis of the error of the horizontal feature point coordinate revealed the interrelationship between the image noise  $\sigma_n^2$ , the local image content, given by the local image intensity values  $I(x, y)$ , and the variance of the feature point's horizontal coordinate error  $\sigma_\Delta^2$ . A formula for the disparity error variance based on the feature coordinate error variance has been derived. In an experiment (section 4) it was shown that the results of the analytical derivation match measured results obtained using synthetic images and images from a real camera. A second experiment has shown that the coordinate error variance of feature points at a full-pel position is smaller by a factor of three than that for feature points at half-pel position.

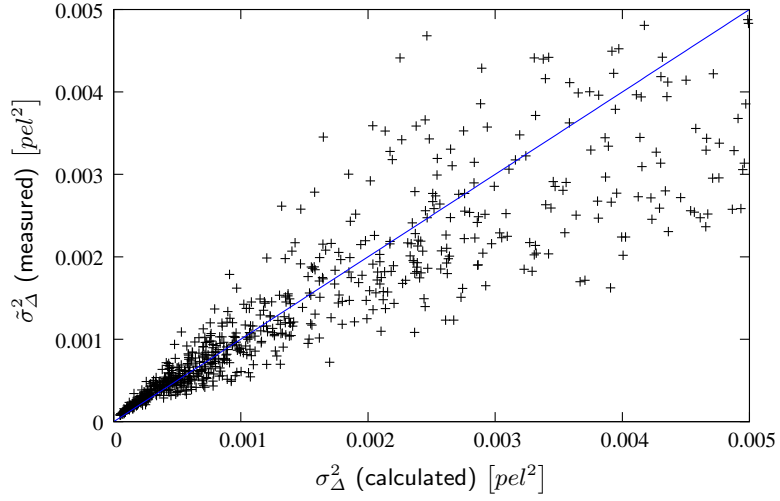


**Fig. 3.** Measured error variances  $\tilde{\sigma}_{\Delta}^2$  over analytically calculated error variances  $\sigma_{\Delta}^2$  for each feature point in the image sequence taken with a real camera.



**Fig. 4.** Synthetic image used in the experiment. The edge is slightly slanted, so that feature points with a range of subpel coordinates can be detected.

The calculation presented in this paper allows to benchmark feature points and disparities during feature detection on their expected error variance. This is a great advantage compared to methods that try to eliminate bad feature points at a later stage in the process of disparity estimation.

In the future this work will be expanded to a feature detector that measures gradients in all directions in the image, i.e. the feature detector of Harris et. al.[9]

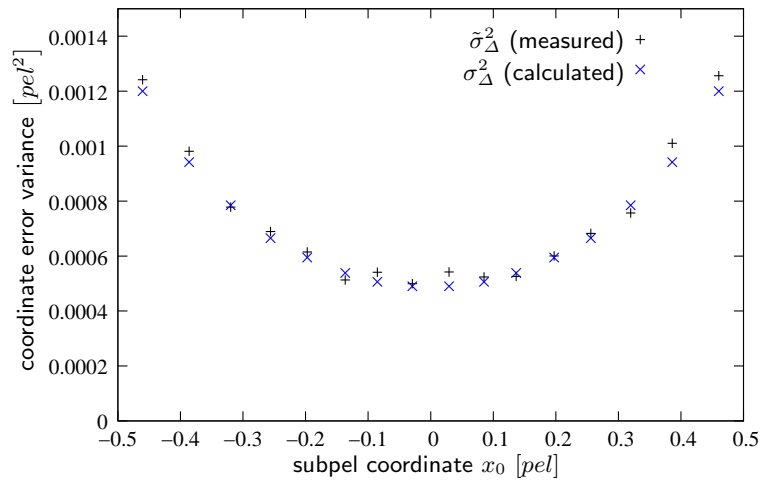


**Fig. 5.** Measured error variance  $\tilde{\sigma}_\Delta^2$  and calculated error variance  $\sigma_\Delta^2$  as function of the subpel coordinate  $x_0$ .

## References

1. Luxen, M.: Variance component estimation in performance characteristics applied to feature extraction procedures. In Michaelis, B., Krell, G., eds.: Pattern Recognition, 25th DAGM Symposium, Magdeburg, Germany, September 10-12, 2003, Proceedings. Volume 2781 of Lecture Notes in Computer Science., Springer (2003) 498–506
2. Rohr, K.: Localization properties of direct corner detectors. *Journal of Mathematical Imaging and Vision* 4 (1994) 139–150
3. Szeliski, R.: Bayesian Modeling of Uncertainty in Low-Level Vision. Kluwer International Series in Engineering and Computer Science, 79, ISBN: 0792390393 (1989)
4. Shi, J., Tomasi, C.: Good features to track. In: CVPR, IEEE (1994) 593–600
5. Kanazawa, Y., Kanatani, K.: Do we really have to consider covariance matrices for image features? In: ICCV. (2001) 301–306
6. Morris, D.D., Kanade, T.: A unified factorization algorithm for points, line segments and planes with uncertainty models. In: Proceedings of Sixth IEEE International Conference on Computer Vision (ICCV'98). (1998) 696–702
7. Singh, A.: An estimation-theoretic framework for image-flow computation. In: ICCV. Third international conference on computer vision (1990) 168–177
8. Förstner, W.: Reliability analysis of parameter estimation in linear models with applications to mensuration problems in computer vision. In: CVGIP 40. (1987) 273–310
9. Harris, C., Stephens, M.: A combined corner and edge detector. In: 4th Alvey Vision Conference. (1988) 147–151